rapid switch from low to high external calcium concentration applied to the chimaera first results in a potentiation of the ionic current, followed by a decline of response amplitude due to channel block (Fig. 3*b*). Also, in support of the potentiating effect of calcium on the chimaera, a slight increase of EC_{50} for ACh from 36 μM at 0.01 mM external calcium to 25 μM at 2.5 mM external calcium is noticed (Fig. 3*e*). These data show that the large N-terminal domain of the nicotinic α7 receptor not only contains the neurotransmitter binding site, but also the allosteric site(s) for calcium.

Thus, functional properties that are expected to be determined by the extracellular domain on one hand, or by the channel domain on the other hand, are found to be associated with the corresponding protein segment in the chimaera. In contrast, the kinetics of current onset and desensitization, which are both rapid in α7WT and slow in $5HT_3$WT, are intermediate in the chimaera (Figs 1 and 2). This suggests that the rates of interconversion between the multiple conformational states of a given ligand-gated ion channel (for both activation and desensitization) involve the tertiary and quaternary structure of the whole receptor molecule rather than a restricted structural domain.

Distinct functional properties of two members among the superfamily of the ligand-gated ion channels can thus be combined into a new chimaeric α7–$5HT_3$ receptor by the exchange of homologous sequence elements. This allows us to assign, without ambiguity, neurotransmitter binding and Ca^{2+} allosteric properties to the large N-terminal hydrophilic domain, and ionic channel properties to the other moiety. But the successful coupling of the neurotransmitter binding site from one receptor to the ion channel from the other supports the additional notion of at least two independent protein domains with folding autonomy[32] and functional specificity, which behave as elementary units within the ligand-gated channel complex. Moreover, their ability to interact functionally, despite the low sequence homology of the receptors from which they originate, suggests that the different members of the ligand-gated ion channels superfamily share a highly conserved architectural framework designed to mediate signal transduction. □

Received 25 August; accepted 5 October 1993.

1. Couturier, S. *et al. Neuron* **5,** 845–856 (1990).
2. Schoepfer, R., Conroy, W. G., Whiting, P., Gore, M. & Lindstrom, J. *Neuron* **5,** 35–48 (1990).
3. Maricq, A. V., Peterson, A. S., Brake, A. J., Myers, R. M. & Julius, D. *Science* **254,** 432–437 (1991).
4. Bertrand, D., Bertrand, S. & Ballivet, M. *Neurosci. Lett.* **146,** 87–90 (1992).
5. Séguéla, P., Wadiche, J., Dineley-Miller, K., Dani, J. A. & Patrick, J. W. *J. Neurosci.* **13,** 596–604 (1993).
6. Bertrand, D., Galzi, J. L., Devillers-Thiéry, A., Bertrand, S. & Changeux, J. P. *Proc. natn. Acad. Sci. U.S.A.* **90,** 6971-6975 (1993).
7. Mulle, C., Léna, C. & Changeux, J. P. *Neuron* **8,** 937–945 (1992).
8. Vernino, S., Amador, M., Luetje, C. W., Patrick, J. & Dani, J. A. *Neuron* **8,** 127–134 (1992).
9. Peters, J. A., Hales, T. G. & Lambert, J. J. *Eur. J. Pharm.* **151,** 491–495 (1988).
10. Dennis, M. *et al. Biochemistry* **27,** 2346–2357 (1988).
11. Galzi, J. L. *et al. J. biol. Chem.* **265,** 10430–10437 (1990).
12. Kuhse, J., Schmieden, V. & Betz, H. *Neuron* **5,** 867–873 (1990).
13. Vandenberg, R. J., French, C. R., Barry, P. H., Shine, J. & Schofield, P. R. *Proc. natn. Acad. Sci. U.S.A.* **89,** 1765–1769 (1992).
14. Sigel, E., Baur, R., Kellenberger, S. & Malherbe, P. *EMBO J.* **11,** 2017–2023 (1992).
15. Karlin, A. *Curr. Opin. Neurobiol.* **3,** 299–309 (1993).
16. Claudio, T., Ballivet, M., Patrick, J. & Heinemann, S. *Proc. natn. Acad. Sci. U.S.A.* **80,** 1111–1115 (1983).
17. Devillers-Thiéry, A., Giraudat, J., Bentaboulet, M. & Changeux, J. P. *Proc. natn. Acad. Sci. U.S.A.* **80,** 2067–2071 (1983).
18. Noda, M. *et al. Nature* **301,** 251–255 (1983).
19. Giraudat, J., Dennis, M., Heidmann, T., Chang, J. Y. & Changeux, J. P. *Proc. natn. Acad. Sci. U.S.A.* **83,** 2719–2723 (1986).
20. Hucho, F., Oberthür, W. & Lottspeich, F. *FEBS Lett.* **205,** 137–142 (1986).
21. Imoto, K. *et al. Nature* **324,** 670–674 (1986).
22. Mayne, K. M., Yoshii, K., Yu, L., Lester, H. A. & Davidson, N. *Molec. Brain Res.* **2,** 191–197 (1987).
23. Yu, X. M. & Hall, Z. W. *Nature* **352,** 64–67 (1991).
24. Sumikawa, K. *Molec. Brain Res.* **13,** 349–353 (1992).
25. Bradley, P. B. *et al. Neuropharmacology* **25,** 563–576 (1986).
26. Higashi, H. & Nishi, S. *J. Physiol., Lond.* **323,** 543–567 (1982).
27. Yakel, J. L., Lagrutta, A., Adelaman, J. P. & North, R. A. *Proc. natn. Acad. Sci. U.S.A.* **90,** 5030–5033 (1993).
28. Yang, J., Mathie, A. & Hille, B. *J. Physiol., Lond.* **448,** 237–256 (1992).
29. Miledi, R. & Parker, I. *J. Physiol.* **357,** 173–183 (1984).
30. Galzi, J. L. *et al. Nature* **359,** 500–505 (1992).
31. Yang, J. *J. Gen. Physiol.* **96,** 1177–1198 (1990).
32. Popot, J. L. & Engelman, D. *Biochemistry* **29,** 4031–4037 (1990).
33. Higuchi, R., Krummel, B. & Saiki, R. K. *Nucleic Acids Res.* **16,** 7351–7367 (1989).
34. Swick, A. G., Janicot, M., Cheneval-Kastelic, T., McLenithan, J. C. & Lane, M. D. *Proc. natn. Acad. Sci. U.S.A.* **89,** 1812–1816 (1992).
35. Bertrand, D., Cooper, E., Valera, S., Rungger, D. & Ballivet, M. *Electrophysiology of Neuronal Nicotinic Acetylcholine Receptors Expressed in* Xenopus *Oocytes Following Nuclear Injection of Genes or cDNA* 1-174-193 (Academic, San Diego, 1991).

ACKNOWLEDGEMENTS. This work was supported by grants from the Association Français contre les Myopathies, the Collège de France, the Centre National de la Recherche Scientifique, the Ministère de la Recherche, the Direction des Recherches Etudes et Techniques, the Commission of the European Communities, the International Human Frontier Science Program, and the Swiss National Science Foundation, OFES and Sandoz Foundation (to D.B.). J.L.G. is a recipient of a short-term EMBO fellowship.

The crystal structure of a two zinc-finger peptide reveals an extension to the rules for zinc-finger/DNA recognition

Louise Fairall, John W. R. Schwabe, Lynda Chapman, John T. Finch & Daniela Rhodes

MRC Laboratory of Molecular Biology, Hills Road, Cambridge CB2 2QH, UK

THE Cys_2-His_2 zinc-finger is the most widely occurring DNA-binding motif[1–3]. The first structure of a zinc-finger/DNA complex revealed a fairly simple mechanism for DNA recognition[4] suggesting that the zinc-finger might represent a candidate template for designing proteins to recognize DNA[5]. Residues at three key positions in an α-helical 'reading head' play a dominant role in base-recognition and have been targets for mutagenesis experiments aimed at deriving a recognition code[6–8]. Here we report the structure of a two zinc-finger DNA-binding domain from the protein Tramtrack complexed with DNA. The amino-terminal zinc-finger and its interaction with DNA illustrate several novel features. These include the use of a serine residue, which is semi-conserved and located outside the three key positions, to make a base contact. Its role in base-recognition correlates with a large, local, protein-induced deformation of the DNA helix at a flexible A-T-A sequence and may give insight into previous mutagenesis experiments[9,10]. It is apparent from this structure that zinc-finger/DNA recognition is more complex than was originally perceived.

Tramtrack (TTK) is a transcriptional regulator of the *Drosophila* development gene *fushi-tarazu*[11,12]. The 66-residue DNA-binding domain (TTKDBD) contains two zinc-finger motifs with 10 residues (3 encoded by the vector) N-terminal to the conventional start of the first zinc-finger[13]. The crystal structure of the TTKDBD with an 18-base-pair (bp) oligonucleotide (Fig. 1*a*) was solved to 2.8 Å by isomorphous replacement (Table 1). The two zinc-finger motifs form independent DNA-binding modules (Fig. 1*b*), each positioned with the N terminus of an α-helix pointing into the major groove and making base-specific contacts. Most of the protein–DNA contacts are made to one strand of the binding site (Fig. 1*a*). The binding sites for the two fingers overlap. The alignment of the protein on its binding site and a number of the amino-acid to base contacts agree with our predictions based on footprinting analyses[13].

Although the structure of finger 1 of TTK (and its interaction with DNA) shows several unanticipated features (see below), the structure of finger 2 is essentially the same as seen previously for other zinc-fingers[4,14–16] (see legend to Fig. 1). Furthermore, finger 2 binds to DNA in a very similar manner to each of the three fingers of Zif268, with residues in equivalent positions making similar base and phosphate contacts (Fig. 3). Arg 152 and Asn 155 each make bidentate contacts to G8 and A7, respec-

TABLE 1 Statistics from the crystallographic analysis

Position of thymine substituted		Native	16	5	28
Resolution		2.8 Å	2.8 Å	3.2 Å	3.1 Å
Reflections total/unique		43,552/11,994	42,582/11,775	25,494/7,946	24,762/7,252
Multiplicity		3.6	3.6	3.2	3.4
Completeness		99.2%	99.3%	98.8%	82.4%
R_{merge}		5.6% (2.87–2.8 Å 31.2%)	5.1% (2.87–2.8 Å 33.2%)	8.7% (3.37–3.2 Å 13.5%)	9.8% (3.26–3.1 Å 22.3%)
F/σ		41.9 (2.83–2.8 Å 9.65)			
Mean fractional isomorphous difference (3.3–3.2 Å)			6.4 (9.1)	11.4 (15.2)	13.6 (18.3)
MIR analysis 20–3.2 Å (3.57–3.24 Å):					
Phasing power	centric		0.5 (0.3)	0.8 (0.5)	0.5 (0.2)
	acentric		0.8 (0.6)	1.1 (0.8)	0.7 (0.5)
R-Cullis			0.77 (0.97)	0.67 (0.89)	0.83 (0.95)
Mean overall figure of merit	centric	0.69 (0.50)			
	acentric	0.46 (0.28)			

The protein and DNA used to obtain crystals are shown in Fig. 1*a*. The purification of the protein, the identification of an oligonucleotide sequence recognized specifically by the TTKDBD and the preparation of complex have been described previously[13]. For crystallization trials, a 1:1 complex was concentrated from ~15 μM to 0.3 mM. Crystals were grown in small tubes at 20 °C with a final complex concentration of between 0.075 and 0.15 mM in a buffer containing 20 mM MES pH 6, 5–20 mM NaCl and 1.75–3.5 mM spermine. Ordered native crystals could be grown from solution only once and further native and derivative crystals (using 5-bromouridine-substituted oligonucleotides) were grown by micro-seeding from one of the original crystals. Crystals grew to a maximum size of 200 × 400 × 600 μm. They were stabilized by the addition of MPD (2-methyl-2,4-pentanediol) to 2% before mounting for data collection, and diffract to 2.8 Å at room temperature. The crystals are in the space group $P2_12_12_1$ with cell dimensions of 60.7 × 64.6 × 117.6 Å. The asymmetric unit contains two molecules of complex (two protein molecules and two DNA duplexes). Native and derivative data were collected using MAR (Hamburg, Germany) image plate scanners, both in our laboratory and at the Daresbury synchrotron source (station 9.5). These data were processed using IPMOSFLM[21], merged using the CCP4 suite of programs[22] and phases were calculated using MLPHARE[23]. A solvent-flattened[24] MIR electron density map at 3.2 Å showed clear density for the DNA and 90% of the protein. A starting model of the complex based on the Zif268 structure and DNase I footprinting data for Tramtrack[13] made map fitting straightforward. This was done using the graphics program O[25]. The DNA was globally positioned in the map based on the coordinates of the bromine atoms in the derivatives and then individual bases were repositioned to give a better fit. The protein was positioned globally in a similar way by locating the high-intensity density for the zinc atoms and aligning the secondary structure in the model with the skeletonized density produced by the program BONES[26] implemented in O[25]. The DNA molecules are packed end to end in the crystals by forming base triples: the terminal overhanging pyrimidine in one duplex makes a Hoogsteen interaction with the purine of the terminal base pair of the next duplex. The model was initially refined using X-PLOR[27]. In early rounds the DNA was strongly constrained to maintain base planarity and pairing using the parameter file parallhdg.dna, but these constraints were relaxed towards the end of the refinement using the parameter file param11x.dna (ref. 27). Multiple rounds of rebuilding and refinement in X-PLOR were followed by refinement using TNT[28]. Certain residues or side-chains were found to be poorly ordered in one or other or both of the complexes and have been omitted from the final model. These include: Met 101, Glu 102, Arg 114, Ser 117, Asn 137, Lys 165 and Ile 166. The current model contains 63 water molecules and has a *R* factor of 19.8% with r.m.s. deviation from ideal geometry of 0.015 Å in bond lengths and 2.14° in bond angles. The r.m.s. deviation between the B values of covalently bonded atomic pairs is 2.75 Å^2.

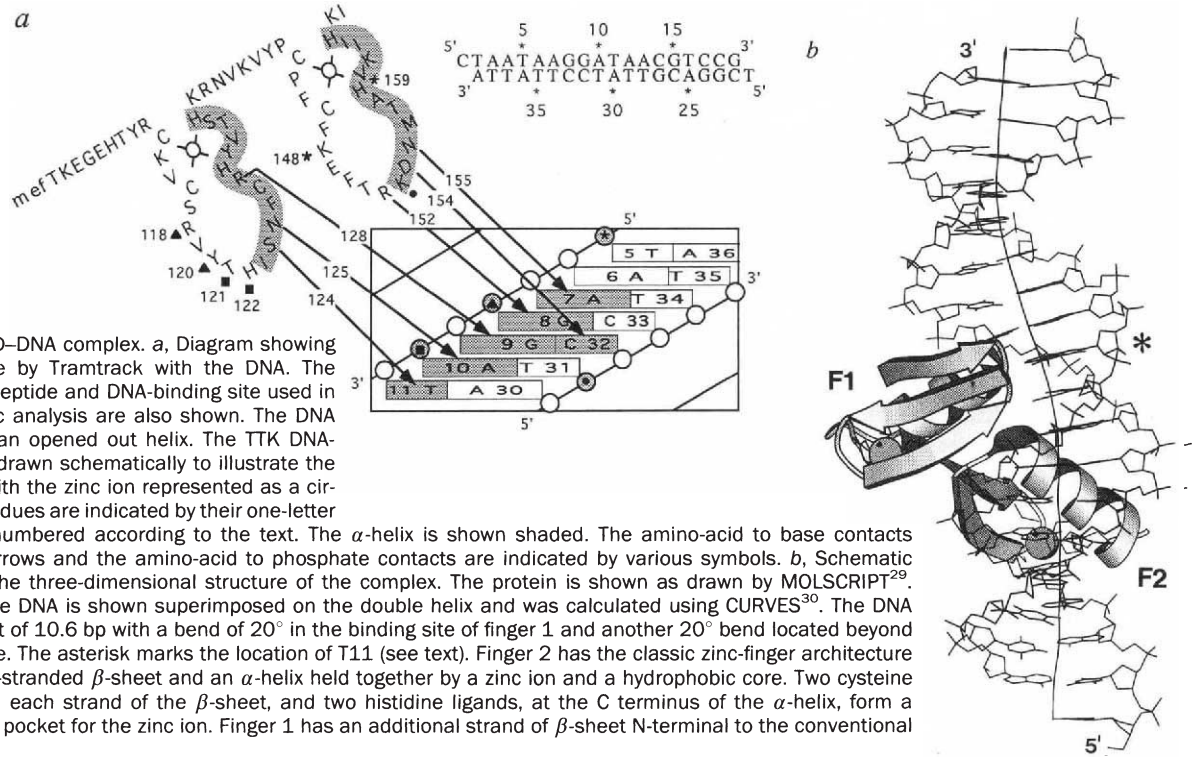

FIG. 1 The TTKDBD–DNA complex. *a*, Diagram showing the contacts made by Tramtrack with the DNA. The sequences of the peptide and DNA-binding site used in the crystallographic analysis are also shown. The DNA is represented as an opened out helix. The TTK DNA-binding domain is drawn schematically to illustrate the zinc-finger motif, with the zinc ion represented as a circle. Amino-acid residues are indicated by their one-letter abbreviation and numbered according to the text. The α-helix is shown shaded. The amino-acid to base contacts are indicated by arrows and the amino-acid to phosphate contacts are indicated by various symbols. *b*, Schematic representation of the three-dimensional structure of the complex. The protein is shown as drawn by MOLSCRIPT[29]. The helix axis of the DNA is shown superimposed on the double helix and was calculated using CURVES[30]. The DNA has a helical repeat of 10.6 bp with a bend of 20° in the binding site of finger 1 and another 20° bend located beyond the TTK binding site. The asterisk marks the location of T11 (see text). Finger 2 has the classic zinc-finger architecture consisting of a two-stranded β-sheet and an α-helix held together by a zinc ion and a hydrophobic core. Two cysteine ligands, located on each strand of the β-sheet, and two histidine ligands, at the C terminus of the α-helix, form a tetrahedral binding pocket for the zinc ion. Finger 1 has an additional strand of β-sheet N-terminal to the conventional zinc-finger.

tively. Asp 154 accepts two buttressing hydrogen bonds from Arg 152 and makes a good hydrogen bond to C32 on the opposite strand of the DNA. Such a contact was seen for finger 2 of Zif268, but had an unfavourable geometry. His 159, one of the zinc ligands, and Lys 148, from the second β-strand, both contact the phosphate 5P. Lys 153 in the α-helix contacts a phosphate (31P) across the major groove (Fig. 1*a*).

The residues linking the two finger domains have a high average temperature factor, indicating that this region is rather flexible or disordered. Hence the orientation of each finger domain is determined by the protein–DNA contacts and is unlikely to be influenced by the structure of the linker.

The structure of finger 1 shows that the residues N-terminal to the conventional finger motif fold to form a third strand to the β-sheet (Fig. 2*a*), in a similar way to the first zinc-finger of the protein SW15 (ref. 17). The additional β-strand, which is required for binding to DNA, is not seen to interact directly with DNA and is thus probably required for the structural stability of finger 1.

Several features of the interaction of finger 1 with DNA were unexpected. First, the zinc–histidine–phosphate 'charge relay' contact, observed in all three fingers of Zif268 and finger 2 of TTK, is substituted in finger 1 by a tyrosine–phosphate contact (Tyr 120 to 8P) (Fig. 2*b*). This variation is particularly interesting because the metal-binding histidine is invariant and had been assumed to serve as a phosphate anchor in all zinc-finger domains. The β-strand N-terminal to the α-helix makes many more contacts to the phosphate backbone than had been seen before (Arg 118 to 8P, Tyr 120 to 8P, Thr 121 to 10P and His 122 to 10P) and this is probably a consequence of a bend in the DNA (see below).

Second, the DNA in the crystal is deformed with a bend of 20° towards the protein in the binding site of finger 1 (Fig. 1*b*). This bend occurs at the readily deformable sequence A-T-A (ref. 18) (A10-T11-A12). The A-T and T-A steps have twists of 24° and 40°, respectively. Although alternate low and high twist are characteristic of this sequence[19], the twist of the A-T step is particularly low and results in the bases of T11 and A10 stacking

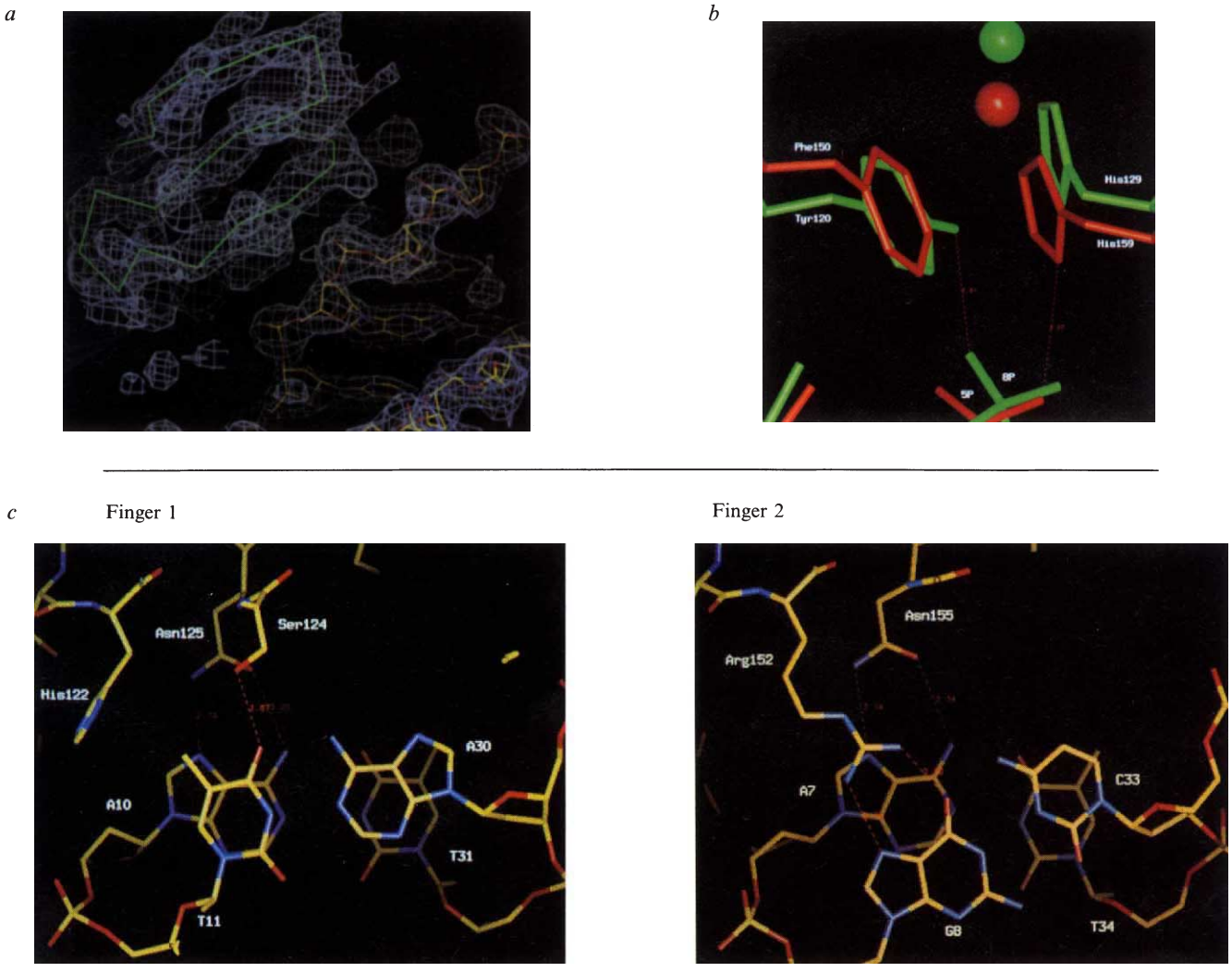

FIG. 2 Finger 1 has several features that are different from finger 2. *a*, The three β-strands of finger 1 shown in the $2F_o-F_c$ electron density map contoured at 0.3 electrons Å^{-3}. This view also shows the phosphate backbones of the DNA and some of the base pairs in the minor groove. *b*, The histidine–phosphate contact observed in finger 2 (red), and the 3 fingers of Zif268, is substituted by a tyrosine–phosphate contact in finger 1 (green). *c*, The distortion of the DNA helix (shown in Fig. 1) results in a displacement of T11 in the binding site of finger 1 towards the protein so that the base is within hydrogen-bonding distance of Ser 124. The amino-acid to base contacts for corresponding positions in the binding sites of fingers 1 and 2 are shown.

directly over each other. Consequently, T11 is displaced towards the protein by 2.5 Å compared with the equivalent base in the binding site for finger 2 (Fig. 2*c*). This permits the short side-chain of Ser 124 to interact with the O4 of T11. The distortion at base pair T11-A30 appears to be due to protein binding because in solution the N3 of A30 is reactive to dimethyl sulphate, but only when bound to protein[13]. This deformation illustrates that DNA need not be a passive partner in the recognition process[18].

Finally, the pattern of amino acid/base contacts observed for finger 1 of TTK differs from that seen for finger 2 and the three fingers of Zif268 (Fig. 3*c*). A striking feature of the Zif268 structure was that it implied a general mechanism for zinc-finger/DNA recognition. In each finger, amino acids at three key positions (termed −1, 3 and 6 in Fig. 3*c*) have the potential to make base contacts to one strand of the DNA. The residues at positions −1 and either 3 or 6 make contacts to bases at positions A and either B or C within a base triplet, respectively. This general mechanism was supported by a statistical analysis of a large number of zinc-finger sequences[2]. Consequently, residues at these three key positions have been the focus of mutagenesis studies aimed at deriving a set of general rules for zinc-finger/DNA recognition[6–8].

Finger 1 of TTK, unlike finger 2, does not conform to these simple rules (Fig. 3*c*). The histidine at position −1 is used to make a phosphate, rather than a base contact. Residues at key positions 3 and 6 make base contacts: Asn 125 to A10 (position 3 to B) and Arg 128 to G9 (position 6 to C) (Fig. 3*a*). Ser 124, in an additional position, 2, makes a third base contact to T11 at position A. Notably, serine is conserved at this position in over 50% of zinc-finger sequences[2]. In several of the TTK binding sites the thymine T11 is substituted by a cytosine[11,12,20].

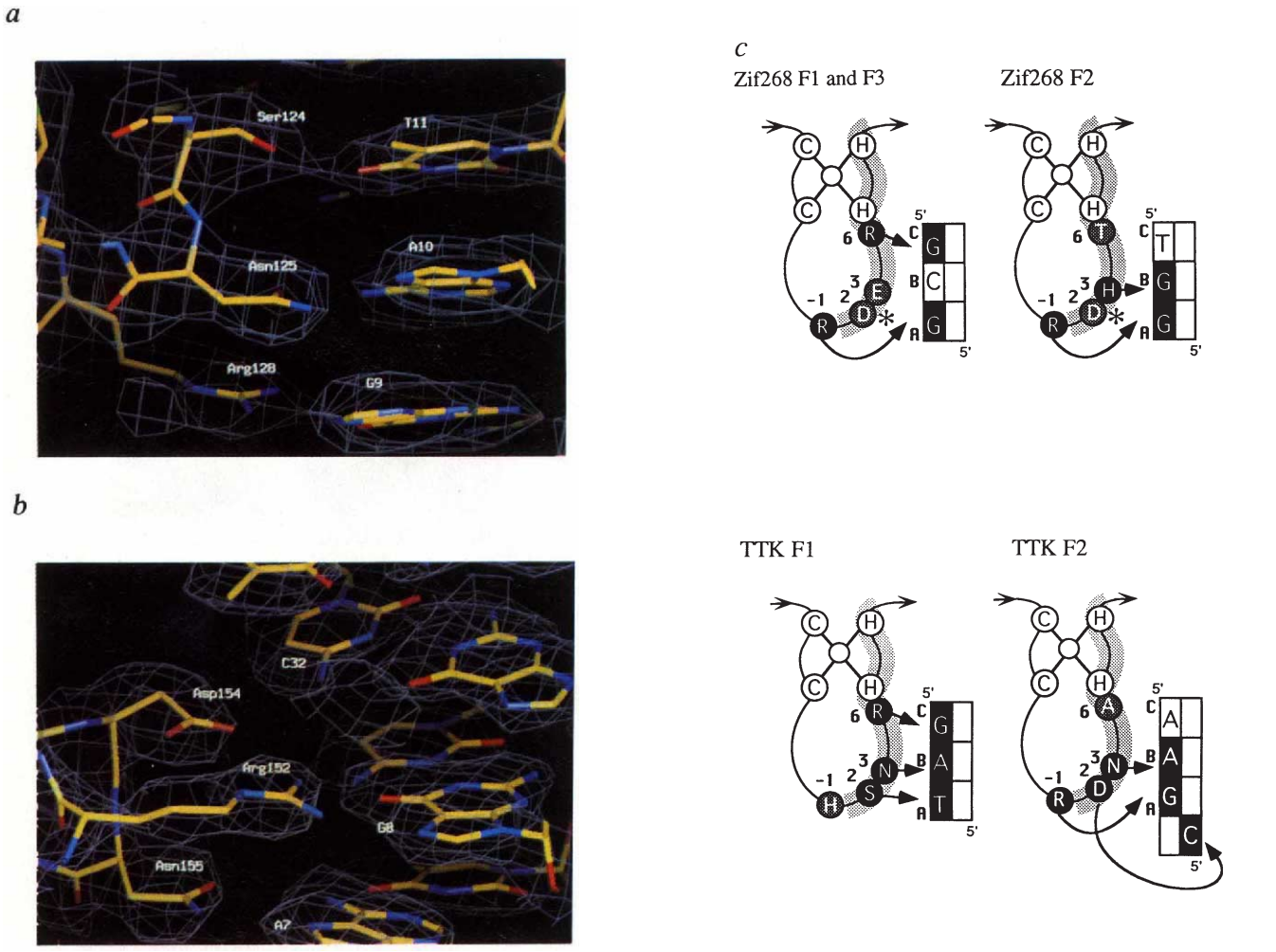

FIG. 3 The base-specific contacts made by the two zinc-fingers of Tramtrack. *a*, Base contacts of finger 1 shown in the $2F_o-F_c$ electron density map contoured at 0.3 electrons Å^{-3}. From top to bottom Ser 124 contacts T11, Asp 125 contacts A10 and Arg 128 contacts G9. *b*, Base contacts of finger 2 shown in the $2F_o-F_c$ electron density map contoured at 0.3 electrons Å^{-3}. From top to bottom Asp 154 buttresses Arg 152 and contacts C32, Arg 152 contacts G8 and Asn 155 contacts A7. All the base contacts for finger 1 and finger 2 are made to one strand of the DNA with the exception of the contact to C32. *c*, Patterns of contacts in the three fingers of Zif268 (F1, F2 and F3) and the two fingers of TTK (F1 and F2) to their respective base triplets. The amino-acid to base contacts are shown as white letters on a black background with arrows joining them. The four positions in the protein used for making base contacts are labelled −1, 2, 3 and 6 with the positions not used shown on a dark grey background. The positions are numbered according to the start of the α-helix. The three positions of the base triplet are labelled A, B and C. The location of the α-helix is indicated by the light grey shaded area. The asterisks mark the aspartic acids which make contacts to a base on the other strand of the DNA for the Zif268 fingers but were considered unimportant as described in the text.

Presumably a rotation about the Cβ–Oγ bond would allow the serine to accept a hydrogen bond from N4 of the cytosine with no overall change in the geometry of the interaction. Substitution of the thymine by a cytosine, but not by a purine, should permit the DNA deformation described above. Hence it may emerge that fingers with a serine at position 2 have the potential to recognize a pyrimidine in position A, but this would probably require a deformation of the DNA.

It has been proposed from mutagenesis data that a glutamine in position −1 may recognize a thymine in position A (refs 9, 10). But to obtain such recognition, it was necessary to mutate additional residues: position 2 to a serine and position 3 to an aspartic acid[9,10]. In the light of the TTK structure, we suggest that an alternative interpretation is possible: the serine, and not the glutamine, is contacting the thymine, and the glutamine would then be in a suitable position to make a phosphate contact. This alternative interpretation is supported by Nardelli *et al.* who had difficulty modelling the proposed glutamine to thymine contact because they found that only a long side-chain at position −1, such as that of arginine, could reach the DNA bases[8].

In conclusion, the TTK structure reveals an extension to the pattern of direct protein–DNA contacts derived from the Zif268 structure. It remains to be seen whether further structures of zinc-finger/DNA complexes will reveal additional rules for zinc-finger DNA recognition. Establishing such rules is important if we are to design successfully zinc-finger proteins to recognize predetermined DNA sequences.

Finally, a recent structure determination[31] supports our conclusions that not all zinc-fingers exhibit the same pattern of protein–DNA contacts seen for Zif268. The differences in this structure are greater than those between TTK and Zif268, but because three of the five fingers in this structure make virtually no contacts to DNA, it may be that this protein is atypical. □

Received 6 August; accepted 15 October 1993.

1. Miller, J., McLachlan, A. D. & Klug, A. *EMBO J.* **4,** 1609–1614 (1985).
2. Jacobs, G. H. *EMBO J.* **11,** 4507–4517 (1992).
3. Hoovers, J. M. N. *et al. Genomics* **12,** 254–263 (1992).
4. Pavletich, N. P. & Pabo, C. O. *Science* **252,** 809–817 (1991).
5. Berg, J. M. *Curr. Opin. struct. Biol.* **3,** 11–16 (1993).
6. Desjarlais, J. R. & Berg, J. M. *Proc. natn. Acad. Sci. U.S.A.* **89,** 7345–7349 (1992).
7. Desjarlais, J. R. & Berg, J. M. *Proc. natn. Acad. Sci. U.S.A.* **90,** 2256–2260 (1993).
8. Nardelli, J., Gibson, T. J. & Charnay, P. *Nucleic Acids Res.* **20,** 4137–4144 (1992).
9. Desjarlais, J. R. & Berg, J. M. *Proteins* **12,** 101–104 (1992).
10. Desjarlais, J. R. & Berg, J. M. *Proteins* **13,** 282 (1992).
11. Harrison, S. D. & Travers, A. A. *EMBO J.* **9,** 207–216 (1990).
12. Brown, J. L., Sonoda, S., Ueda, H., Scott, M. P. & Wu, C. *EMBO J.* **10,** 665–674 (1991).
13. Fairall, L., Harrison, S. D., Travers, A. A. & Rhodes, D. *J. molec. Biol.* **226,** 349–366 (1992).
14. Lee, M. S., Gippert, G. P., Soman, K. V., Case, D. A. & Wright, P. E. *Science* **245,** 635–637 (1989).
15. Klevit, R. E., Herriott, J. R. & Horvath, S. J. *Proteins* **7,** 215–226 (1990).
16. Omichinski, J. G., Clore, G. M., Appella, E., Sakaguchi, K. & Gronenborn, A. M. *Biochemistry* **29,** 9324–9334 (1990).
17. Neuhaus, D., Nakaseko, Y., Schwabe, J. W. R. & Klug, A. *J. molec. Biol.* **228,** 637–651 (1992).
18. Travers, A. A. & Klug, A. in *DNA Topology and its Biological Effects* (eds Cozzarelli, N. R. & Wang, J. C.) 57–106 (Cold Spring Harbor Laboratory Press, New York, 1990).
19. Yoon, C., Prive, G. G., Goodsell, D. S. & Dickerson, R. E. *Proc. natn. Acad. Sci. U.S.A.* **85,** 6332–6336 (1988).
20. Read, D. & Manley, J. L. *EMBO J.* **11,** 1035–1044 (1992).
21. Leslie, A. G. W. In *Joint CCP4 and ESF-EACBM Newsletter on Protein Crystallography* Number 26 (Daresbury Laboratory, Warrington, UK, 1992).
22. *CCP4* The SERC (UK) Collaborative Computing Project No. 4, a suite of Programs for Protein Crystallography (Distributed from the Daresbury Laboratory, Warrington, UK, 1979).
23. Otwinowski, Z. in *Isomorphous Replacement and Anomalous Scattering* 80–86 (Daresbury Laboratory, Warrington, UK, 1991).
24. Leslie, A. G. W. *Acta crystallogr.* A**43,** 134–136 (1987).
25. Jones, T. A., Zou, J.-Y., Cowan, S. W. & Kjeldgaard, N. *Acta crystallogr.* A**47,** 110–119 (1991).
26. Greer, J. *Meth. Enzym.* **115,** 206–224 (1985).
27. Brünger, A. T. *X-PLOR* v. 3.0 manual (Yale Univ., New Haven, 1992).
28. Tronrud, D. E., Ten Eyck, L. F. & Matthews, B. W. *Acta crystallogr.* A**43,** 489–501 (1987).
29. Kraulis, P. *J. appl. Crystallogr.* **24,** 946–950 (1991).
30. Lavery, R. & Sklenar, H. *J. biomolec. struct. Dynam.* **6,** 655–667 (1989).
31. Pavletich, N. P. & Pabo, C. O. *Science* **261,** 1701–1707 (1993).

ACKNOWLEDGEMENTS. We thank P. Evans and A. Leslie for their advice on many aspects of data collection and processing, T. Horsnell and K. Henrick for their help in compiling TNT, T. Smith and J. Fogg for oligonucleotide synthesis and A. Klug, A. Travers, Y. Choo, J. Li and W. Scott for comments on this manuscript. This work was in part supported by the Human Frontier Science Program.